

PERFORMANCE OF SUSCEPTOR MATERIALS IN HIGH FREQUENCY MAGNETIC FIELDS

*Russell J. Nichols, Drew P. LaMarca, and Bryan Agosto
Ashland Specialty Chemical Co.*

Abstract

Joining of thermoplastics by electromagnetic implant welding is a mature process, yet little information is found in the literature to describe the relationship between the properties of magnetic susceptor particles, the plastic matrix materials in which they are dispersed, and their interaction with high frequency electromagnetic fields.

Magnetic implant welding uses susceptors that couple, due to ferromagnetic hysteresis, with high frequency electromagnetic radiation to generate controllable heat in the plastic. The relationship of coupling distance, power level, and frequency to the heating response of susceptors is studied.

Conclusions are presented, based on the results of statistically designed experiments, that suggest optimal conditions for effective welding processes.

Background

The EMABOND[®] process¹ was introduced over thirty years ago, and has enjoyed continuing success in welding pressure vessels and other highly demanding thermoplastic components that require robust structural, hermetic, and aesthetically pleasing joints. First popularized for its effective solution for joining low surface energy polymers such as polypropylene and polyethylene, its use has broadened over the past decade to include the full range of engineering thermoplastics and highly filled compounds that are difficult to join by other methods.

Electromagnetic Principles

Faraday's law of induction defines the relationship between electric fields and magnetic fields as follows [1]:

$$\mathcal{E} = \frac{-d\Phi_B}{dt} \quad (1)$$

where

\mathcal{E} is the electromotive force (emf) in volts

Φ_B is the magnetic flux in webers

For the case of a coil of wire, comprised of N loops with the same area, Faraday's law of induction states that

$$\mathcal{E} = -N \frac{d\Phi_B}{dt} \quad (2)$$

where

\mathcal{E} is the electromotive force (emf) in volts

N is the number of turns of wire

Φ_B is the magnetic flux in webers through a single loop

The minus sign found in equations 1 and 2 is from Lenz's law, and shows that the direction of the induced emf and the current it drives around the circuit opposes the change in the applied magnetic flux.

Magnetic flux is the product of the magnetic flux density B (in tesla) times the area A perpendicular to the field:

$$\Phi_B = BA \quad (3)$$

The magnetic flux density, or average magnetic field B , is dependent upon the number of turns N in a coil and the current I (in amperes):

$$B \propto NI \quad (4)$$

As shown in Figure 1A, integrating around a closed path gives the amp-turns linking with the path, so for simple systems:

$$NI = \oint H \cdot dI = 2\pi rH \quad (5)$$

where H is the magnetic field strength (Ampere/meter)

$$H = \frac{NI}{2\pi r} \quad (6)$$

Volume magnetization, M , is a vector quantity that represents the density of net magnetic dipole moments, μ in the material:

$$M = \mu_{total} / V \quad (7)$$

and is related to the total magnetic field B in the material by:

$$B = B_0 + \mu_0 M \quad (8)$$

¹ © Registered trademark of Ashland

where μ_0 is the magnetic permeability of space and B_0 is the externally applied magnetic field.

When the magnetic field strength H is plotted against the resultant flux density B in a ferromagnetic material, as in Figure 1B, it forms a closed S-shaped loop. The heat generated due to hysteresis loss is proportional to the area bounded by the curve, and is a result of the properties of the magnetic material. Bozorth [2] gives the rise in temperature during one complete hysteresis cycle for annealed iron as being about 0.0003°C . Thus it is evident that the rate of heating caused by hysteresis is directly dependent upon frequency as well as the quality of the magnetic material.

The physics of electromagnetic induction applies to both Joule heating (eddy current losses) and magnetic heating (hysteresis losses). Benatar [3] describes the heating of ferromagnetic susceptor materials as a combination of both of these effects. He also explains that the current density diminishes rapidly with increasing penetration depth, a well known phenomena in induction heat treating of steel.

It is not within our present technical capability to directly measure the proportions to which these heating effects contribute to the total heating of the susceptor material, nor were we able to measure effective penetration depth. However, we can create a schematic representation in which the magnetic contribution and the eddy current (Joule) heating are displayed as separate factors, as in Figure 1C, with the overall heating effect being the vector sum of the two individual contributors. In some cases, it is intuitively obvious which mechanism dominates; non-conductive, but ferromagnetic materials (e.g., ceramic ferrites) respond only to magnetic hysteresis, while conductive, but non-magnetic materials (e.g., aluminum flakes) respond to eddy currents (Joule heating) while remaining unaffected by the magnetic field. In the case of iron-based ferromagnetic materials, both magnetic hysteresis and eddy current heating contribute significantly to heating, but Nichols [4] has suggested that eddy current development is likely to be inhibited by the insulating matrix of polymer surrounding the iron particles.

High Frequency System Elements

The basic implant welding system is comprised of four primary components: a high-frequency generator, a work coil (the "antenna" that transmits the energy to the susceptor material placed in the bond line), a press to hold the parts in place during the weld cycle, and a cooling system to control the temperature of the work coil and selected generator components.

The tube-type high frequency generator most commonly used for plastic welding incorporates three primary functions: (1) a circuit that controls the sequential functions of the generator, including a PLC that interfaces

with all other system components; (2) a power supply circuit, including an SCR input voltage controller, a plate transformer that steps up the input voltage to 4,000 to 8,000 volts AC, and a full wave rectifier to convert the high voltage AC to DC at the same potential; and (3) an oscillator circuit that uses a vacuum amplifier tube to sustain the oscillation frequency determined by the tank circuit by replenishing the energy lost to the process with energy from the power supply. The tank circuit consists of large capacitors in parallel with the work coil.

Standard parameters monitored include load and grid current. The principle advantage of the oscillator tube technology is that it is very robust and quite insensitive to significant shifts in inductive load (a common effect of flow and displacement of iron-filled implant materials during welding).

Alternatively, high frequency energy can be produced by solid-state generators in which devices such as MOSFET's (metal-oxide semiconductor field-effect transistors) are used instead of oscillator tubes to convert the AC input power to the high frequency, pulsed DC output. In this type of generator, the frequency is fixed by the generator circuitry, and therefore a matching network is required to match the impedance of the generator output to that of the work coil. The control circuitry of the solid state systems can be significantly more complex than that used for oscillator tube systems, but offers more sophisticated control possibilities. Measurement of system operating parameters may include the voltage delivered to the coil and forward and reflected power.

Implant Welding Process Description

Figure 2A shows the FLIR thermal imaging camera used in this study. Figure 2B is an x-ray of a typical susceptor strand showing the way susceptor particles are suspended in the polymer matrix strands. As previously described by Nichols, [5] electromagnetic radiation absorbed by the ferromagnetic particles embedded in the polymer matrix material causes the susceptor particles to rapidly heat. Conductive heat transfer from the ferromagnetic particles into the polymer matrix material causes creeping flow of the implanted material. Under modest pressure the implant material fills the joint cavity, and conductive heat transfer between the implant material and the substrate surfaces causes molecular bonding when sufficient pressure is applied to fully compress the joint surfaces and eliminate void space.

Experimental Plan

Unlike previous studies by Stokes [6], and Wu [7], which investigated the strength of induction welded parts without detailed study of the underlying heating mechanism, these tests focused solely on the heating characteristics of the susceptor materials. The study employed the most widely used magnetic susceptor and

polymer system, iron particles in polypropylene extruded strand, 0.23 mm diameter. Two high frequency generators were used, an Ashland model HD-500 5 kilowatt oscillator tube system operating at 5.5 MHz, and a Seren model AT50/140 5 kilowatt solid state system operating at 13.56 MHz. Heating response was measured using a FLIR Systems Thermacam model A40 long wave focal plane array (FPA) thermal analysis package.

A Taguchi L18 orthogonal array was selected for the experimental design because it was only possible to evaluate frequency at two levels, while coupling distance and coil voltage were evaluated at three levels. The frequency level of 13.56 MHz is a fixed characteristic of the solid state system, but in the case of the oscillator tube generator, frequency is dependent upon the interaction of the work coil and the capacitance of the tank circuit, which in this example resulted in 5.5 MHz. The same work coil was used throughout the experimental study on both generators. Figure 2C shows the way that the work coil is arranged on the oscillator tube generator, and demonstrates the way that the sample was positioned relative to the work coil. Figure 3A shows the matching network and work coil arrangement as used in this study.

Results and Discussion

In this work, we explore certain fundamental relationships that make the implant electromagnetic welding process function. There are many other parameters worthy of investigation, but not within our present investigational capability.

Table 1 presents the matrix results of the Taguchi L18 design for temperature response at a representative value of 3.5 seconds. The temperature response as a function of time at the extremes in voltage and frequency are shown in Figure 3B. The upper bound of the thermal imaging camera used was 580°C. Figure 4A is a Pareto chart of the main effects, and demonstrates that the dominant factor is frequency, followed by coupling distance (note the minus sign indicating an inverse effect), and coil voltage. From the electromagnetic equations, one would expect that the effects of frequency and coil voltage would be linear (if I and B are constant), while the effect of coupling distance should follow the inverse square law [7]. Figure 4B shows that temperature varies with coupling distance as a power law function. The thermal interaction with the polymer may explain the deviation from the expected inverse square law, but also we could not measure the coil current, I . The distinction between the relative slopes of two frequencies is probably related to the difference in heat absorption by the crystalline polymer at temperatures above and below the melting point. Figure 5A demonstrates that the effect of voltage is linear within reasonable experimental error. Figure 6B is the response surface at 13.56 MHz frequency, and although at this scale difficult to see,

shows that the effect of coil voltage is linear and that of coupling distance is not linear.

Conclusions

The historical basis for optimizing a high frequency implant welding process has been by direct experimentation. This work is viewed as the first step toward a heuristic model to predict welding behavior of materials in known magnetic fields. There are some formidable barriers; the most significant variable, current in the work coil, cannot be measured with our current technology, and our understanding of the interactions between the magnetic susceptor compounds in the magnetic field is far from complete. A significant area, not addressed in this work, is to understand more fully the flow of the susceptor compound in the joint during the welding cycle.

As a larger body of information on the response of various magnetic susceptor compositions in magnetic fields of differing intensity grows, we expect to develop some model laws that will assist in the development and implementation of new applications. The role of thermal imaging is a critical contributor to this new understanding, as for the first time, we have the ability to make a precise measurement of heating during the heating cycle.

Acknowledgements

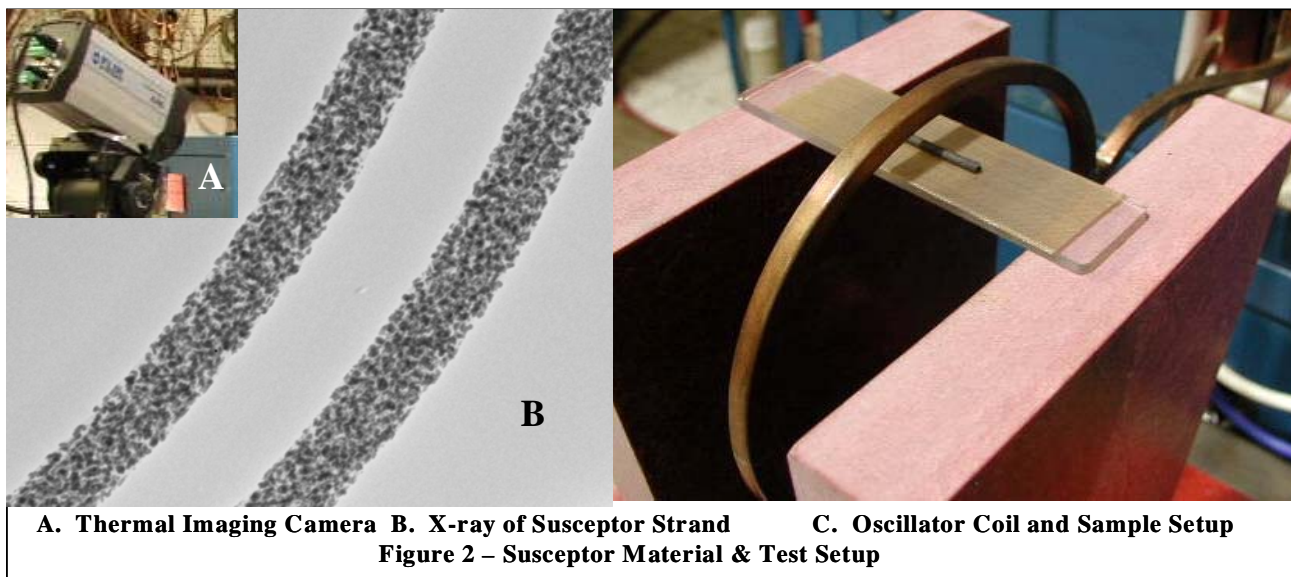
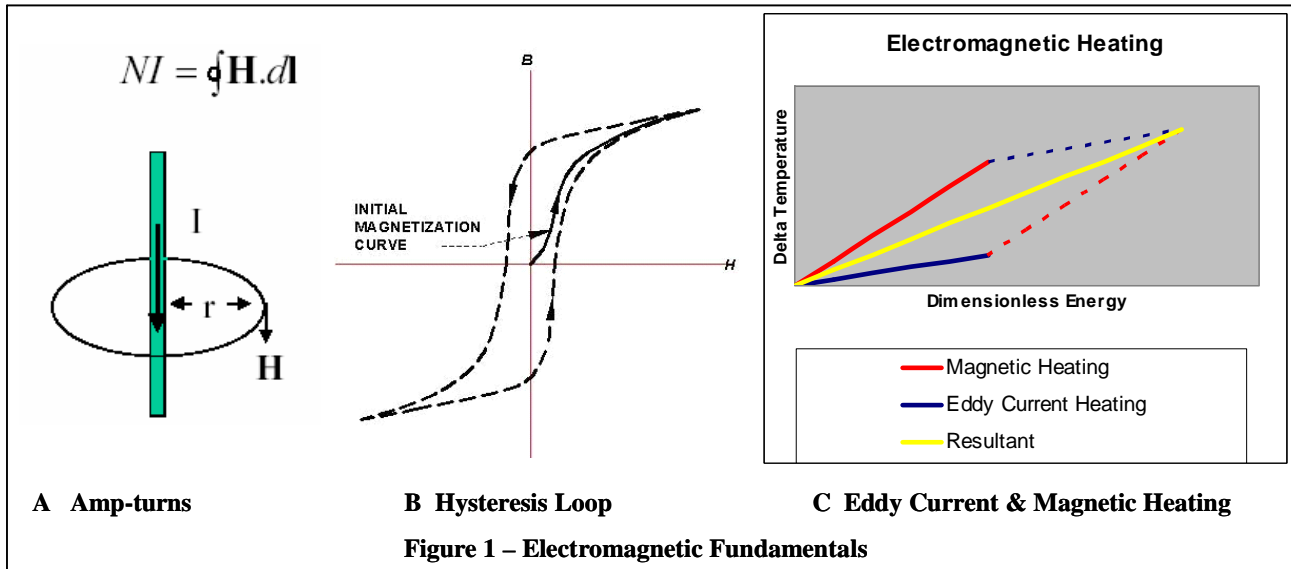
The authors wish to express their appreciation to electrical engineer Clifford Ehrman for his assistance in describing the power supplies.

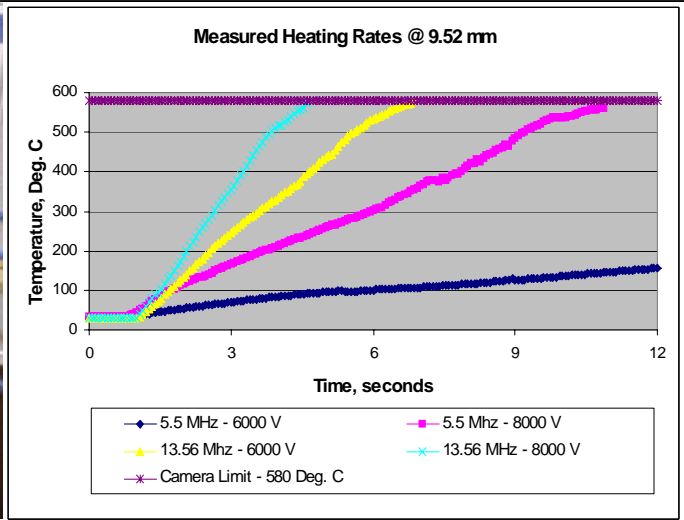
References

1. Retrieved from "http://en.wikipedia.org/wiki/Electromagnetic_induction" 11/6/05
2. R. M. Bozorth, *Ferromagnetism*, IEEE Press, NY, pp.518 (1993) Note: this is a re-issued edition of the 1951 classic published by Van Nostrand Co. Inc.
3. D. A. Grewell, A. Benatar, J. B. Park, *Plastics and Composites Welding Handbook*, Hanser Publishers, Munich, pp. 110-112 (2003)
4. R. J. Nichols, *Advances in the Emabond™ Induction Welding Process for High-Performance Assembly of Demanding Thermoplastics*, Assembly Technology Expo Seminar, (2003)
5. R. J. Nichols, V. A. Kagan, *Induction Welding Takes New Aim for Reinforced Thermoplastics in High Strength and Load Bearing Applications*, SPE ANTEC 2004, p1251
6. V. J. Stokes, *Experiments on the Induction Welding of Thermoplastics*, SPE ANTEC 2001, p. 1288
7. C. Y. Wu, B. Agosto, *Implant Induction Welding of Nylon 6/6*, SPE ANTEC 2005, p. 1039
8. W. H. Hayt, Jr., J. A. Buck, *Engineering Electromagnetics Seventh Edition*, McGraw-Hill, New York, pp 91-92 (2006)

Matrix Results at 3.5 Seconds - Taguchi L18 Design									
Coil Voltage, Volts	6000	6000	6000	7000	7000	7000	8000	8000	8000
Coupling Distance, mm	6.35	9.52	12.7	6.35	9.52	12.7	6.35	9.52	12.7
Run	1	2	3	4	5	6	7	8	9
Temperature, °C (at 5.5 MHz)	92.7	76.6	68.3	211	147.5	138.3	245.5	188.2	146.2
Run	10	11	12	13	14	15	16	17	18
Temperature, °C (at 13.56 MHz)	433.5	289.9	199.4	509.1	328.7	256.6	580.1	440.5	330

Table 1

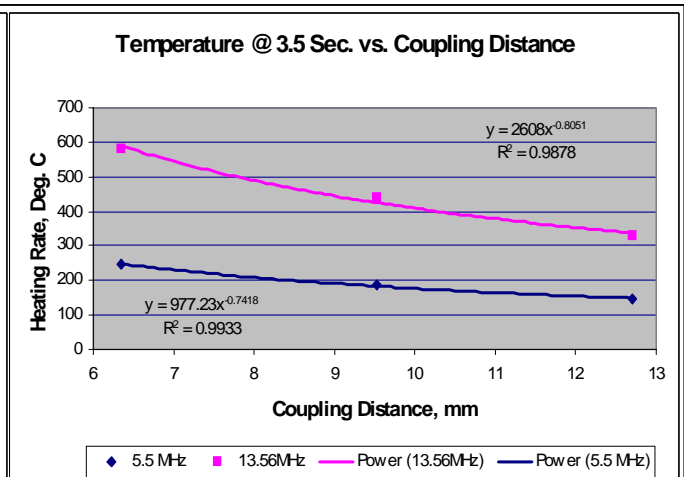
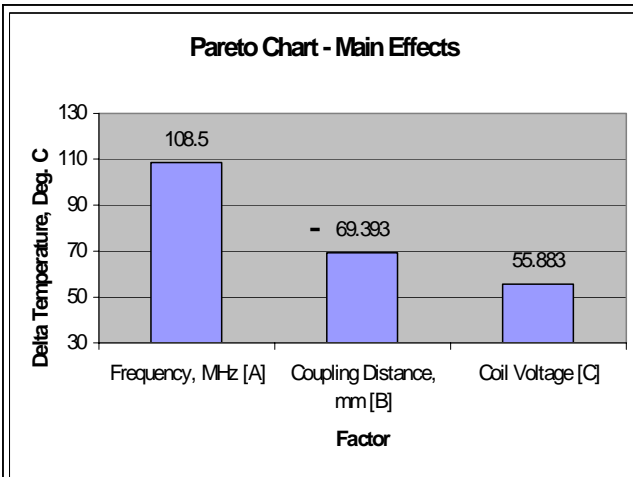




A. Solid State Matching Network & Coil

B. IR Heating Rate Measurement

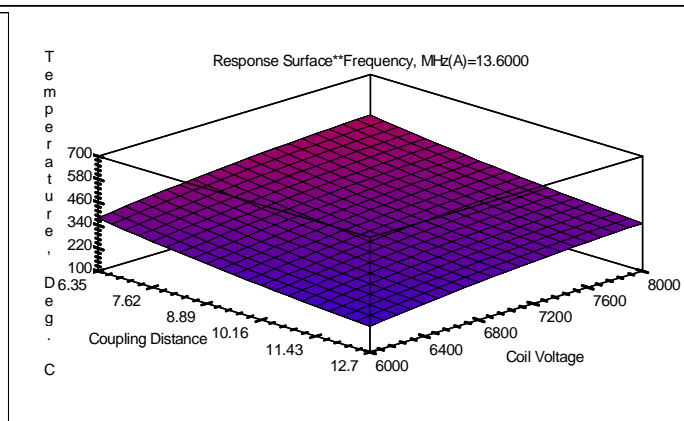
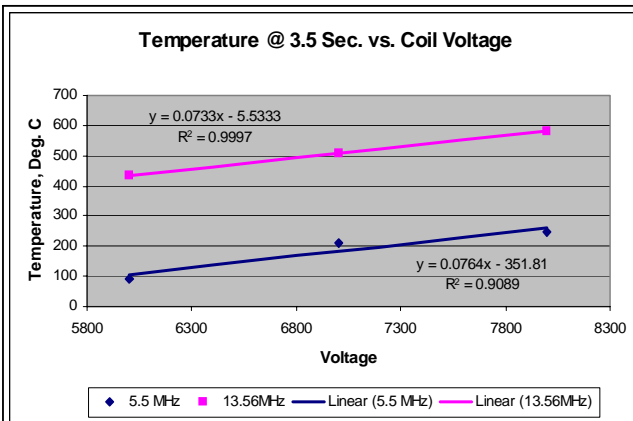
Figure 3 Solid State Matching Network and IR Heating Rate Measurement



A. Pareto Chart – Main Effects

B. Temperature vs. Coupling Distance

Figure 4 – Experimental Results



A –Temperature vs. Coil Voltage

B – Response Surface, @ Frequency = 13.56 MHz

Figure 5 – Experimental Results